PCCP

Cite this: *Phys. Chem. Chem. Phys.*, 2011, **13**, 14163–14175

www.rsc.org/pccp

PAPER

Weak interactions in ion–ligand complexes of $C_3H_3^+$ isomers: competition between H-bound and C-bound structures in c-$C_3H_3^+$·L and H_2CCCH^+·L (L = Ne, Ar, N_2, CO_2, and O_2)†

Peter Botschwina,*[a] Rainer Oswald[a] and Otto Dopfer[b]

Received 18th March 2011, Accepted 11th May 2011
DOI: 10.1039/c1cp20815b

Explicitly correlated coupled cluster theory at the CCSD(T)-F12*x* level (T. B. Adler, G. Knizia, and H.-J. Werner, *J. Chem. Phys.* **127**, 221106, 2007) has been employed to study structures and vibrations of complexes of type c-$C_3H_3^+$·L and $H_2C_3H^+$·L (L = Ne, Ar, N_2, CO_2, and O_2). Both cations have different binding sites, allowing for the formation of weak to moderately strong hydrogen bonds as well as "C-bound" or "π-bound" structures. In contrast to previous expectations, the energetically most favourable structures of all $H_2C_3H^+$·L complexes investigated are "C-bound", with the ligand bound to the methylenic carbon atom. The theoretical predictions enable a more detailed interpretation of infrared photodissociation (IRPD) spectra than was possible hitherto. In particular, the bands observed in the range 3238–3245 cm^{-1} (D. Roth and O. Dopfer, *Phys. Chem. Chem. Phys.* **4**, 4855, 2002) are assigned to essentially free acetylenic CH stretching vibrations of the propargyl cation in "C-bound" $H_2C_3H^+$·L complexes.

1. Introduction

Complexes between a cation containing hydrogen atoms and an atomic or molecular ligand may form hydrogen bonds (H-bonds) with vastly varying binding energies. A well-known example of very strong H-bonds is provided by the "Zundel-cation", $H_5O_2^+$, where the proton is shared between two water molecules[1,2] and the equilibrium dissociation energy D_e for dissociation into fragments H_3O^+ and H_2O is as high as 143 kJ mol^{-1}.[3] On the other hand, much weaker H-bonds exist between $C_nH_m^+$ ions and ligands without permanent electric dipole moments such as rare-gas (Rg) atoms or important atmospheric molecules like N_2, O_2, or CO_2. In addition to H-bonding, $C_nH_m^+$ ions may offer further attractive binding sites leading to the formation of intermolecular bonds to carbon atoms with positive partial charges (C-bonds) or to the π-electron systems of unsaturated C=C/C≡C bonds or aromatic rings (π-bonds). Thus already dimers composed of simple carbocations and neutral atomic or molecular ligands ($C_nH_m^+$·L) may exhibit complex potential energy surfaces (PESs) with multiple minima of comparable energies.

The current knowledge on $C_nH_m^+$·L complexes results mainly from the combination of infrared photodissociation (IRPD) spectroscopy and quantum chemical calculations (see, *e.g.*, ref. 4–6 for earlier reviews). Of particular interest are cases where the carbocation has more than one isomer, thereby contributing additional complexity to IRPD spectra. Ions of formula $C_3H_3^+$ are an outstanding example of that sort. As is well known, cyclic c-$C_3H_3^+$ may be considered as the smallest aromatic carbocation (see, *e.g.*, ref. 7). A more reactive isomer, the propargyl cation ($H_2C_3H^+$) has been known from mass spectrometric studies for four decades.[8] Early experimental work by Lossing[9] found it to be 1.1 ± 0.1 eV higher in energy than c-$C_3H_3^+$.

About a decade ago, high-resolution IRPD spectra of a variety of size-selected $C_3H_3^+$·L_n clusters (L = Ne, Ar, O_2, N_2, CO_2) were obtained in the C–H stretching range using a pulsed single-mode IR laser with 0.017 cm^{-1} resolution and several precursors for generating $C_3H_3^+$ ions in a plasma beam expansion.[10–12] These spectra were analyzed by comparison with *ab initio* calculations at the MP2 (Møller–Plesset second-order perturbation theory) level and the rather limited spectroscopic data for both isolated $C_3H_3^+$ ions available at that time. Despite their importance, high-resolution spectra at the level of rotational resolution are still lacking for both $C_3H_3^+$ isomers. Low-resolution photoelectron spectra of H_2C_3H isotopomers provide no useful vibrational information,[13,14] and a subsequent zero kinetic energy photoelectron (ZEKE) spectrum[15] was withdrawn recently.[16] First spectroscopic

[a] *Institut für Physikalische Chemie, Universität Göttingen, Tammannstraße 6, 37077 Göttingen, Germany. E-mail: pbotsch@gwdg.de; Fax: +49 551 39-3144; Tel: +49 551 39-3133*
[b] *Institut für Optik und Atomare Physik, Technische Universität Berlin, Hardenbergstrasse 36, 10623 Berlin, Germany*
† Electronic supplementary information (ESI) available. See DOI: 10.1039/c1cp20815b

information on nearly unperturbed c-$C_3H_3^+$ and $H_2C_3H^+$ ions came from Ne matrix isolation studies, reporting however only one single vibrational frequency per species.[17] Significantly, the IRPD spectra of $C_3H_3^+$·L identified for the first time by spectroscopy at the level of partial rotational resolution the existence of c-$C_3H_3^+$ and $H_2C_3H^+$ in the gas phase.[10–12] Few bands observed in the IRPD spectra display rotational fine structure attributed to resolved Q branches of perpendicular transitions of (near) symmetric tops. The analysis of their spacings along with their intensities (nuclear spin statistical weights) provided detailed information about their carriers. For example, the IRPD spectrum of $C_3H_3^+$·N_2 demonstrates unambiguously the presence of planar H-bonded structures of c-$C_3H_3^+$· N_2 and $H_2C_3H^+$·N_2 with C_{2v} symmetry in the molecular beam expansion and thus provides strong evidence for the C_{2v} and D_{3h} symmetry of the equilibrium geometries of isolated $H_2C_3H^+$ and c-$C_3H_3^+$, respectively. As however most transitions in the IRPD spectra of $C_3H_3^+$·L did not exhibit rotational fine structure, the suggested vibrational and isomer assignments had to rely mainly on the MP2 calculations and available spectroscopic data for the isolated ions. Unfortunately, some of the vibrational assignments related to complexes of $H_2C_3H^+$ suffered from comparison with the irreproducible ZEKE spectrum.[15,16]

Recently, Ricks *et al.*[18] produced $C_3H_3^+$ · Ar complexes from the vapor of propargyl bromide seeded in 20 atm of argon and investigated them by IRPD spectroscopy over the wide range of 800–4000 cm^{-1}. Table I of that work lists twelve experimental band positions, ten of which were assigned to $H_2C_3H^+$·Ar and two to c-$C_3H_3^+$ · Ar. In both cases, H-bonded structures of C_{2v} symmetry were assumed for the complexes on the basis of quantum chemical calculations, although it is not clear whether alternative structures of different symmetry had been considered at all. However, very recent explicitly correlated coupled cluster calculations carried out at Göttingen have shown that C-bound structures of C_s symmetry are the lowest-energy minima on the PESs of both $H_2C_3H^+$·Ar and c-$C_3H_3^+$· Ar.[19] Vibrational wavenumbers of the fundamentals of free $H_2C_3H^+$ were calculated by the vibrational configuration interaction (VCI) method and combined with harmonic shifts to arrive at predictions for the ionic complexes.[20] Comparison with the IRPD data[18] led to several reassignments of the observed bands.

These recent calculations reveal that knowledge of the subtle competition between H-bonding to acidic protons and C-bonding to positively charged C atoms is vital for a proper interpretation of the IRPD spectra of $C_3H_3^+$ · L complexes. In the light of this new development, the present work characterizes the PESs of $C_3H_3^+$ · L complexes with L = Ne, Ar, O_2, N_2, CO_2 in order to investigate the competition between H-bonding and C-bonding in these clusters in considerable detail at a high theoretical level. As a result, several of the assignments of the IRPD spectra reported previously[10–12] will be revised.

2. Details of calculations

The explicitly correlated CCSD(T)-F12*x* (*x* = *a*, *b*) methods of Werner and coworkers[21–24] were used in most of the electronic structure calculations of the present work. According to various benchmark studies,[22,23] these are very good approximations to standard CCSD(T)[25] close to the basis set limit, but at much lower computational cost. This results from the much faster convergence of electron correlation effects with respect to the size of the atomic orbital (AO) basis set when non-linear terms are included in the electronic wavefunction that depend explicitly on the interelectronic distances. For details of the CCSD(T)-F12*x* methods and their relationship to related methods of other groups we refer to the literature[26] and restrict ourselves to a few details of the calculations.

Following our recent work on $C_3H_3^+$ · Ar,[19,20] a hybrid AO basis set has been employed. For the weakly polarizable cations, we chose the cc-pV*n*Z-F12 (*n* = D, T, and Q) basis sets of Peterson *et al.*,[27] which were specifically developed for F12 calculations. An important part of long-range interaction of the cations with the neutral ligands is induction, the most important parameter of which is the static electric dipole polarizability of the neutral species. As has been known for about 35 years, the accurate computation of this quantity requires flexible AO basis sets including diffuse s, p, and d functions.[28] While the above basis sets are considerably more flexible in the outer region of atoms and molecules than the corresponding cc-pV*n*Z basis sets,[29] they are still not sufficient to yield polarizabilities with 1% accuracy. *E.g.*, CCSD(T)-F12b calculations with the cc-pVQZ-F12 basis set underestimate the polarizability of the argon atom by as much as 11%. Therefore, the aug-cc-pV*n*Z basis sets of Dunning and coworkers[30] were employed for the ligands. We used the same basis set combinations (cation, ligand) as for $C_3H_3^+$ · Ar.[19,20] They may be denoted as (cc-pV*n*Z-F12, aug-cc-pV(*n* + 1)Z). In the following, the shorthand notation (*n*, *n* + 1) = (D, T), (T, Q), or (Q, 5) will be employed. In the majority of the present calculations, the intermediate basis (T, Q) was used. Note that the basis set chosen for Ar actually includes tight d functions and should properly be termed aug-cc-pV(*n* + d)Z.[31]

In addition to the AO basis sets, CCSD(T)-F12*x* calculations require three sets of auxiliary basis sets. We used the optimized auxiliary basis sets of Yousaf and Peterson in conjunction with the cc-pV*n*Z-F12 and aug-cc-pV*n*Z orbital basis sets, respectively.[32,33] They are required as resolution-of-the identity (RI) sets within the complementary auxiliary basis set (CABS) approach. JKFIT and MP2FIT basis sets[34–36] were chosen according to the recommendations of Yousaf and Peterson.[32,33] Tight thresholds were employed in the CABS construction so that no functions were deleted. Throughout, the CABS singles correction[22] was used to improve the Hartree–Fock reference energies. In most of the calculations, variant *x* = *a* was employed and the contribution of connected triple substitutions were scaled according to the recipe of Werner and coworkers.[22,23] This method is denoted by the acronym CCSD(T*)-F12a. Like in the previous calculations for $C_3H_3^+$ · Ar, the geminal exponent was chosen to be 1.2 a_0^{-1} for the largest basis set and 1.0 a_0^{-1} for the two smaller basis sets.

All electronic structure calculations of the present work have been carried out with the MOLPRO system of *ab initio* programs.[37] Geometry optimizations and harmonic wavenumber calculations have been performed by automatic procedures of MOLPRO or by self-written programs for least-squares

fitting of potential energy surfaces and harmonic vibrational analysis. In order to arrive at predictions for anharmonic cation vibrations of the different complex structures, the harmonic wavenumber shifts from the present work have been combined with the recent VCI results for free $H_2C_3H^+$.[20] For the complexes of type c–$C_3H_3^+$· L, we are primarily interested in predictions for the IR active CH stretching vibrations. This allows us to make use of the neon matrix value for ν_4(c-$C_3H_3^+$) which is expected to differ only slightly from the still unknown gas-phase wavenumber. Both $H_2C_3H^+$ and c-$C_3H_3^+$ are semi-rigid molecules without large-amplitude vibrations. The harmonic approximation in the calculation of intramolecular wavenumber shifts should thus work reasonably well. In the case of weak H-bonds, this approximation may benefit from error compensation since stretch-only and stretch-bend anharmonicity contributions may partly cancel each other.

3. Properties of potential energy surfaces

3.1 Potential energy surface scans

Like in our previous work on the complexes of $C_3H_3^+$ isomers with an argon atom,[19,20] we have first calculated energy profiles for the migration of the ligand around the $C_3H_3^+$ moiety along two different paths (see Fig. 1), with the cation and ligand kept rigid in their equilibrium structures. The latter are provided as ESI.† The energetically more favourable path I proceeds in a plane which is perpendicular to the molecular plane and which contains the single C_2 axis of $H_2C_3H^+$ or one of the three equivalent C_2 axes of c-$C_3H_3^+$. Path II proceeds within the molecular plane of either species. Points on path I or II are characterized by the variables (R^{opt}, θ_1) for path I and (R^{opt}, θ_2) for path II, R being optimized for a given value of θ_1 or θ_2. Here, R is the distance between the Rg nucleus or the center of mass of the ligand molecule and the center of mass of the cation. The angles θ_1 and θ_2 are the angles between the distance vector $\vec{R}$ and the C_2 axis of the cation under consideration, either for the out-of-plane (θ_1) or the in-plane (θ_2) situation. The complexes with the linear molecular ligands are studied under the restriction that their molecular axis is oriented along the direction of the $\vec{R}$ vector. In the following, the resulting profiles will be called radial energy profiles. They display the relative energy of the complex (E_{rel}), taken with respect to the energy of the rigid fragments, as a function of either θ_1 and θ_2.

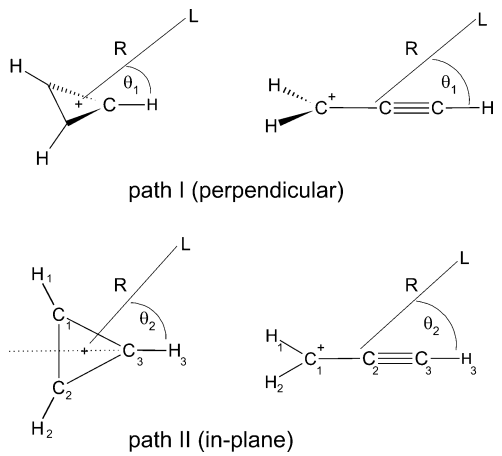

Fig. 1 Description of paths for ligand migration around c-$C_3H_3^+$ and $H_2C_3H^+$.

Radial energy profiles for the complexes c-$C_3H_3^+$·Ne and $H_2C_3H^+$·Ne were studied by CCSD(T*)-F12a with the largest basis set (Q, 5). Results are given in ESI† Tables S1–S4 and are graphically displayed in Fig. 2a–d. Like for the complexes of the two cation isomers with an argon atom,[19] the H-bound structure of C_{2v} symmetry ($\theta_1 = \theta_2 = 0$), termed C_{2v} Min, is only a local minimum on the PES. Along path I, two minima over (R, θ_1) space are lower in energy for c-$C_3H_3^+$·Ne. They are termed C_s Min 1 (lower) and C_s Min 2 (higher). According to the shape of the radial energy profile (2a) one may expect that C_{2v} Min will play a minor role for the IRPD spectrum of c-$C_3H_3^+$·Ne, but owing to the small energy differences over a wide range of angular space, c-$C_3H_3^+$·Ne is probably a rather flexible complex. For $H_2C_3H^+$·Ne, only C_s Min 1 lies below C_{2v} Min. Fig. 2d shows a minimum at $\theta_2 \approx 105°$ at about the same relative energy as for C_{2v} Min. Whether it will be a local minimum in full dimensionality will be investigated below.

Table 1 investigates the basis set dependence of optimum distances and angles (termed R^{opt} and θ_1^{opt}) and the corresponding relative energies for the minima above (R, θ_1) space. The three basis set combinations (D, T), (T, Q), and (Q, 5) are considered. Like for c-$C_3H_3^+$·Ar and $H_2C_3H^+$·Ar (see Tables I and II of ref. 19), already the smallest basis does a remarkably good job. Compared with the results obtained with the large (Q, 5) basis set, the largest difference is only 14 cm^{-1}. The intermediate basis (T, Q) delivers results which differ only slightly (mostly by less than 2 cm^{-1}) from the corresponding results obtained with the (Q, 5) basis set.

Radial energy profiles for c-$C_3H_3^+$·Ar and $H_2C_3H^+$·Ar were published earlier and are not repeated here.[19] Those for the cation–N_2 complexes are shown in Fig. 3a–d; the corresponding ESI† Tables are S5–S8. For c-$C_3H_3^+$·N_2, the lowest energy is

Table 1 Basis set dependence of CCSD(T*)-F12a results for different energy minima of c-$C_3H_3^+$·Ne and $H_2C_3H^+$·Ne[a]

Complex	Structure	Basis set	R^{opt}/Å	θ_1^{opt}/°	E_{rel}/cm^{-1}
c-$C_3H_3^+$·Ne	C_s Min 1	(D, T)	3.3008	62.39	−222.3
		(T, Q)	3.3215	61.83	−210.4
		(Q, 5)	3.3194	62.07	−208.6
	C_s Min 2	(D, T)	3.3061	125.38	−217.9
		(T, Q)	3.3266	125.76	−205.4
		(Q, 5)	3.3188	124.34	−203.4
	C_{2v} Min	(D, T)	4.2260	0	−196.9
		(T, Q)	4.2353	0	−184.9
		(Q, 5)	4.2369	0	−182.9
$H_2C_3H^+$·Ne	C_s Min 1	(D, T)	3.5396	128.85	−252.2
		(T, Q)	3.5501	129.19	−240.9
		(Q, 5)	3.5523	129.16	−239.5
	C_s Min 2	(D, T)	3.5066	54.49	−215.2
		(T, Q)	3.5312	53.98	−204.8
		(Q, 5)	3.5514	53.31	−199.7
	C_{2v} Min	(D, T)	4.6011	0	−221.4
		(T, Q)	4.6154	0	−208.7
		(Q, 5)	4.6185	0	−206.5

[a] Basis sets are described by cardinal number combination (n_1, n_2); see the text. The cations are kept rigid in their equilibrium configuration.

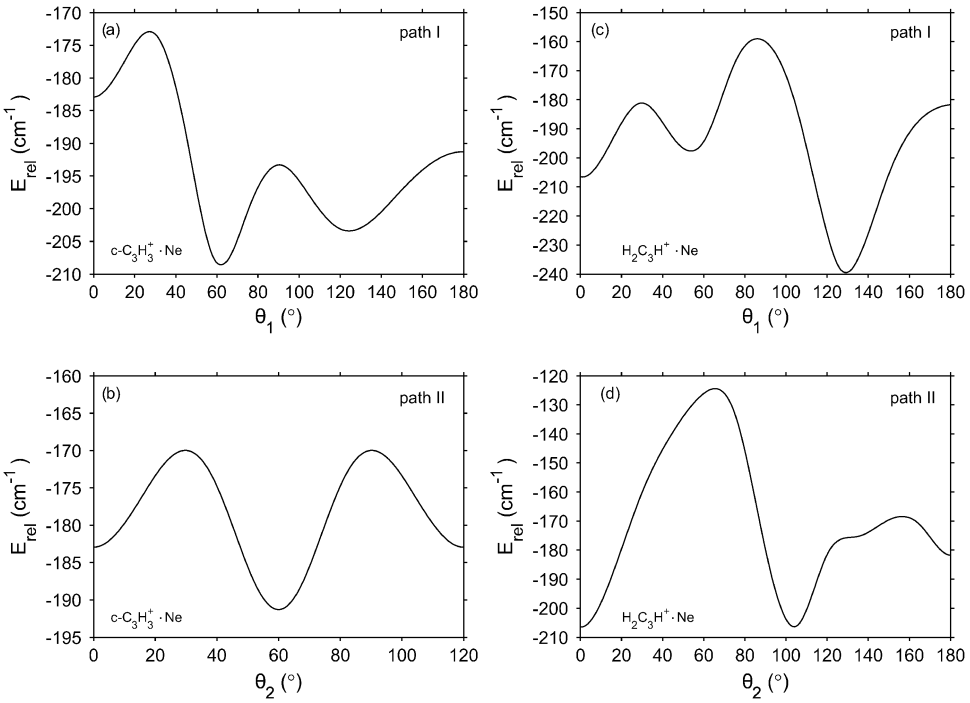

Fig. 2 CCSD(T*)-F12a radial energy profiles for migration of a Ne atom around c-$C_3H_3^+$ or $H_2C_3H^+$. Basis: (Q, 5).

obtained for the H-bound C_{2v} structure, with the C_s minima over (R, θ_1) space lying significantly higher in energy (see Fig. 3a). The latter are expected to play no role for the interpretation of the IRPD spectra. The radial energy profiles for $H_2C_3H^+ \cdot N_2$ are more interesting. The two lowest minima over (R, θ_1) space shown in Fig. 3c are very close in energy and require further optimization in order to decide the question, whether the H-bound structure is the global minimum on the PES. Likewise, the minimum of the radial energy profile for in-plane migration at $\theta_2 \approx 140^\circ$ (see Fig. 3d) deserves further investigation. It might correspond to a H-bonded structure where the ligand is attached to one of the two methylenic H atoms.

Results for the cation–CO_2 complexes are shown in Fig. 4a–d and ESI† Tables S9–S12. For c-$C_3H_3^+ \cdot CO_2$, the H-bound C_{2v} structure ($\theta_1 = \theta_2 = 0$) appears to be favoured over the C-bound structure at $\theta_1 \approx 60^\circ$ (see Fig. 4a). The radial energy profile for perpendicular motion of CO_2 around $H_2C_3H^+$ (see Fig. 4c) shows the lowest relative energy for the C-bound structure. Like for $H_2C_3H^+ \cdot N_2$, the in-plane profile (Fig. 4d) is indicative of a higher-lying local minimum around $\theta_2 = 140^\circ$ in which CO_2 binds to one of the methylenic H atoms.

Finally, Fig. 5 shows the radial energy profile for c-$C_3H_3^+ \cdot O_2$ (path I) in its triplet ground state, calculated by RHF-UCCSD(T*)-F12a.[22] No clear C_{2v} minimum is discernible and the lowest relative energies are calculated in the range $60^\circ \leq \theta_1 \leq 130^\circ$.

3.2 Equilibrium structures and equilibrium dissociation energies

For a variety of complexes of type c-$C_3H_3^+ \cdot$L and $H_2C_3H^+ \cdot$L, equilibrium structures and energies have been calculated by CCSD(T*)-F12a with the intermediate basis set (T, Q). Results for the planar H-bound structures of C_{2v} symmetry (C_{2v} Min) are listed in Tables 2 and 3 along with the changes in equilibrium geometrical parameters with respect to the corresponding values for the free cations. The changes in all CC equilibrium bond lengths are quite small and do not exceed 0.0022 Å. H-bonding leads to an increase in the CH equilibrium bond length r_{2e}, which ranges from only 0.00029 Å for the most weakly bound complex c-$C_3H_3^+ \cdot$Ne to 0.00786 Å for $H_2C_3H^+ \cdot CO_2$. Calculated equilibrium dissociation energies span the wide range between 185 and 2209 cm^{-1}. As is shown in Fig. 6, we find a strongly non-linear relationship between D_e and Δr_{2e} values for both c-$C_3H_3^+ \cdot$L and $H_2C_3H^+ \cdot$L complexes. *E.g.*, the relative changes in Δr_{2e} between L = N_2 and L = CO_2 are much smaller than the relative changes in the corresponding D_e values. This finding is most pronounced for the complexes involving the propargyl cation, where the ratio $\Delta r_{2e}(L = CO_2)/\Delta r_{2e}(L = N_2)$ is only 1.184 while the corresponding ratio for the D_e values is as high as 1.642. An attempt to rationalize this finding is made in Fig. 7. We take the separation between the acetylenic proton and the nucleus of the ligand molecule, termed R_{inter}, as the abscissa variable. Relative energies and the intramolecular geometrical parameters of the cation and the ligand molecule are then optimized. At $R_{inter} = 3.0$ Å, already 55% or 47% of the equilibrium dissociation energies are obtained for L = N_2 or L = CO_2, respectively. At that intermolecular distance, the change in r_2^{opt} with respect to the asymptotic value is still very small for both complexes. Apparently, a large part of D_e is gained through long-range interaction before chemical forces set in to produce significant elongation of the acetylenic CH distance.

According to the results of Tables 2 and 3, the ligand CO_2 experiences substantial changes in its equilibrium bond

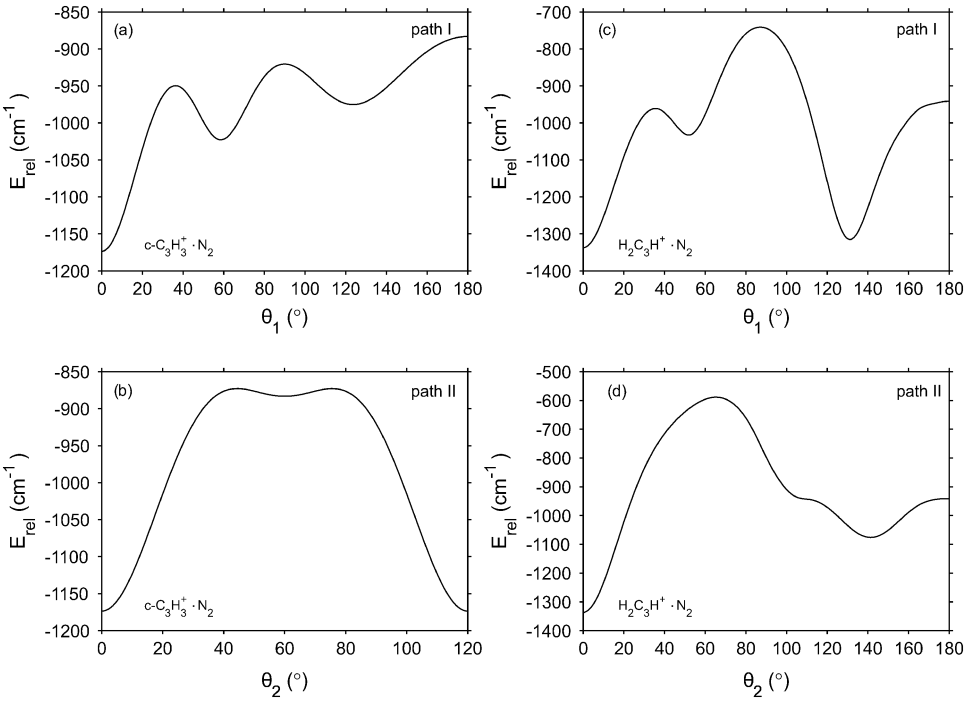

Fig. 3 CCSD(T*)-F12a radial energy profiles for migration of a N_2 molecule around c-$C_3H_3^+$ or $H_2C_3H^+$. Basis: (T, Q).

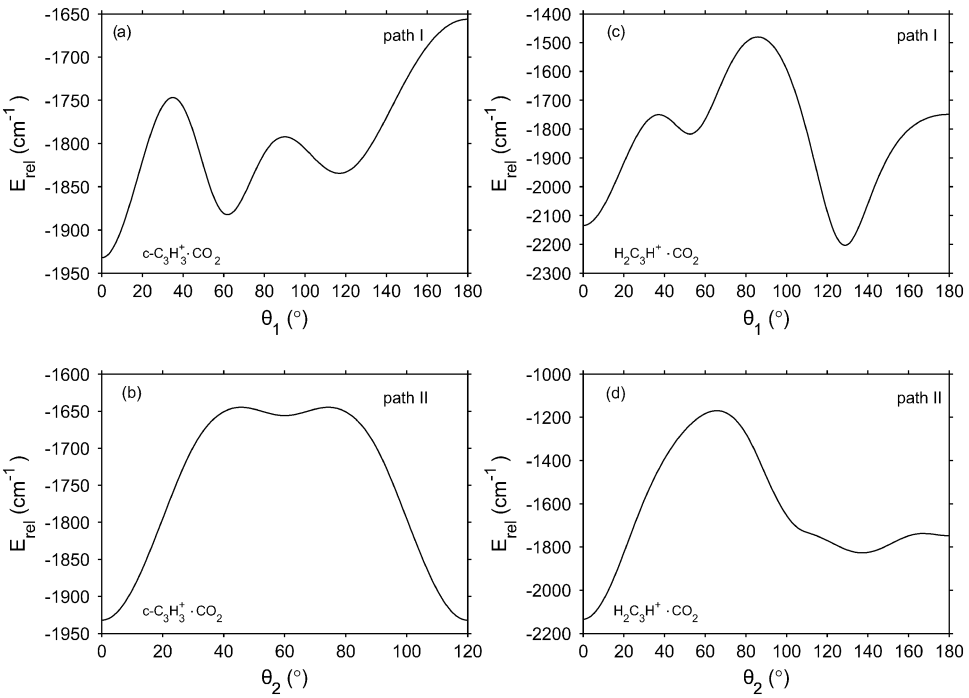

Fig. 4 CCSD(T*)-F12a radial energy profiles for migration of a CO_2 molecule around c-$C_3H_3^+$ or $H_2C_3H^+$. Basis: (T, Q).

lengths. For $H_2C_3H^+ \cdot CO_2$, they are as large as +0.00852 Å (inner CO bond) and −0.00997 Å (outer CO bond). Such an asymmetric distortion produces an electric dipole moment with the proper sign to increase intermolecular attraction. Distortion sets in rather early. Already at R_{inter} = 3.0 Å, the optimum CO distances have changed by +0.00528 and −0.00580 Å, thereby producing an energy lowering of −23.0 cm^{-1}. Distortion of free CO_2 by the same amount requires an energy of 22.9 cm^{-1}.

The lowest energy minima of C_s symmetry for the Rg complexes of c-$C_3H_3^+$ are characterized by equilibrium angles θ_1^e = 61.8° (Ne) and θ_1^e = 62.2° (Ar). The corresponding separations between the centers of mass of the fragments are R_e = 3.322 Å and R_e = 3.558 Å, respectively. For the

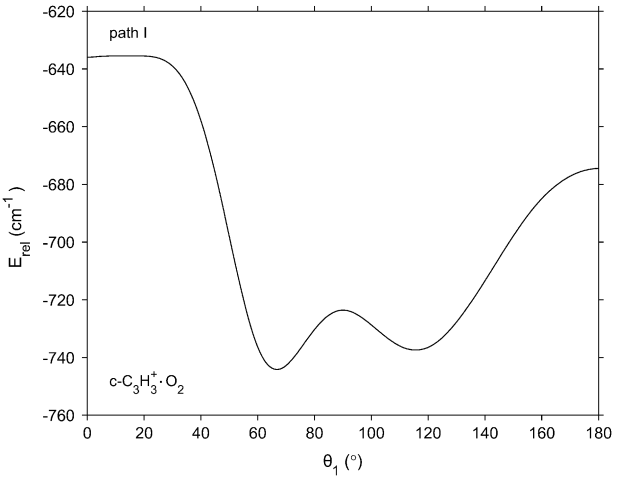

Fig. 5 RHF-UCCSD(T*)-F12a radial energy profiles for migration of an O_2 molecule around c-$C_3H_3^+$ along path I. Basis: (T, Q).

Table 2 CCSD(T*)−F12a equilibrium structures and dissociation energies D_e for H-bound c-$C_3H_3^+$·L (C_{2v} symmetry)[a]

Geometrical parameter[b]	c-$C_3H_3^+$·Ne	c-$C_3H_3^+$·Ar	c-$C_3H_3^+$·N_2	c-$C_3H_3^+$·CO_2
r_{1e}/Å	1.07970	1.07961	1.07945	1.07927
	(−0.00003)	(−0.00012)	(−0.00028)	(−0.00046)
β_e/°	150.00	150.00	149.99	149.98
R_{1e}/Å	1.36301	1.36252	1.36157	1.36085
	(−0.00017)	(−0.00066)	(−0.00161)	(−0.00233)
R_{2e}/Å	1.36337	1.36376	1.36439	1.36482
	(0.00019)	(0.00058)	(0.00121)	(0.00164)
r_{2e}/Å	1.08002	1.08160	1.08373	1.08436
	(0.00029)	(0.00187)	(0.00400)	(0.00463)
R^e_{inter}/Å	2.3689	2.5724	2.2462	2.0081
R^L_{1e}/Å			1.09890	1.17058
			(−0.00048)	(0.00849)
R^L_{2e}/Å				1.15260
				(−0.00949)
D_e/cm^{-1}	184.9	535.2	1177.2	1997.8

[a] Basis: (T, Q). Differences with respect to monomers are given in parentheses. R^e_{inter} is the equilibrium separation between nuclei of atoms involved in H-bonds. [b] Cation geometrical parameters are defined as follows (see bottom of Fig. 1): r_{1e}, R_{1e}, R_{2e}, and r_{2e} refer to equilibrium distances H_1C_1, C_1C_2, C_2C_3, and C_3H_3, respectively, and β_e is the equilibrium $H_1C_1C_3$ angle.

Table 3 CCSD(T*)-F12a equilibrium structures and dissociation energies D_e for H-bound $H_2C_3H^+$·L (C_{2v} symmetry)[a]

Geometrical parameter[b]	$H_2C_3H^+$·Ne	$H_2C_3H^+$·Ar	$H_2C_3H^+$·N_2	$H_2C_3H^+$·CO_2
r_{1e}/Å	1.08743	1.08734	1.08720	1.08707
	(−0.00005)	(−0.00011)	(−0.00025)	(−0.00038)
α_e/°	119.32	119.30	119.26	119.23
	(−0.01)	(−0.03)	(−0.07)	(−0.10)
R_{1e}/Å	1.34929	1.34884	1.34815	1.34747
	(−0.00019)	(−0.00064)	(−0.00133)	(−0.00201)
R_{2e}/Å	1.23127	1.23179	1.23254	1.23312
	(0.00024)	(0.00078)	(0.00153)	(0.00211)
r_{2e}/Å	1.07497	1.07731	1.08094	1.08216
	(0.00067)	(0.00301)	(0.00664)	(0.00786)
R^e_{inter}/Å	2.2918	2.5015	2.1608	1.9359
R^L_{1e}/Å			1.09875	1.17061
			(−0.00063)	(0.00852)
R^L_{2e}/Å				1.15212
				(−0.00997)
D_e/cm^{-1}	241.1	593.9	1344.8	2208.8

[a] Basis: (T, Q). Differences with respect to monomers are given in parentheses. R^e_{inter} is the equilibrium separation between nuclei of atoms involved in H-bonds. [b] Angle α_e is the equilibrium $H_1C_1H_2$ angle, other geometrical parameters are defined as in footnote b of Table 2.

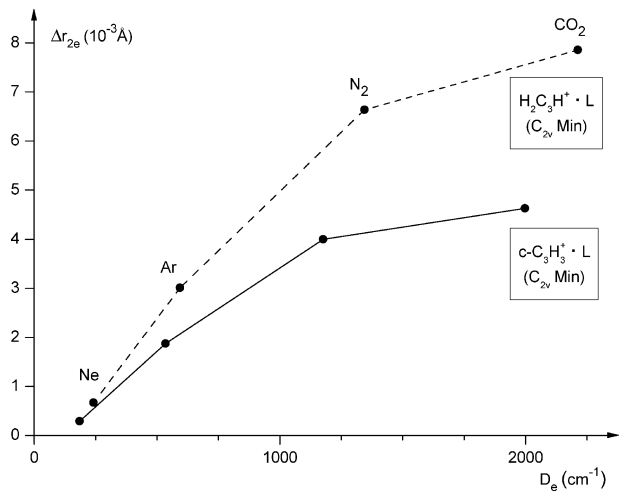

Fig. 6 Correlation between the elongation of the H-bound CH equilibrium bond length and dissociation energy D_e. Results obtained by CCSD(T*)-F12a with basis (T, Q).

complexes $H_2C_3H^+$·Ne and $H_2C_3H^+$·Ar, the combinations (θ_1^e, R_e) have values of (3.550 Å, 129.2°) and (3.568 Å, 126.5°).

Optimized C_s Min 1 structures of the complexes with L = N_2 and L = CO_2 are displayed in Fig. 8. They are called "C-bound" since the shortest distances between ligand nitrogen or oxygen nuclei and carbon nuclei are relatively small, ranging from 2.49 Å for $H_2C_3H^+$·CO_2 to 3.01 Å for c-$C_3H_3^+$·N_2. Changes in intramolecular equilibrium geometrical parameters and dissociation energies D_e are listed in Table 4 (c-$C_3H_3^+$·L) and Table 5 ($H_2C_3H^+$·L). For both cations, all CH equilibrium bond lengths are slightly shortened upon complex formation. This is indicative of slight blue-shifts in all CH stretching vibrational wavenumbers of both cations. Distortions of the carbon framework is somewhat stronger than for the C_{2v} minima, but still rather moderate in the most strongly bound complex $H_2C_3H^+$·CO_2. Here, the CC equilibrium bond lengths are both shortened by *ca.* 0.004 Å.

Results of geometry optimizations for the planar C_s structures of $H_2C_3H^+$·L complexes are graphically displayed in Fig. 9. Center-of-mass intermolecular equilibrium distances (straight lines) are displayed for all complexes. For L = N_2 and L = CO_2, the shortest N···H and O···H equilibrium distances (dotted lines) are quoted as well. Both values are indicative of moderately weak hydrogen bonds. D_e values for three different structures (order from above: C_s planar, C_s Min 2, and C_s Min 1) are also included in Fig. 9 for comparison. Among the planar C_s structures, the great differences between weakly bound cation–rare gas complexes and moderate strongly bound cation–molecule complexes are clearly discernible. For the former, θ_2^e values around 100° were calculated and

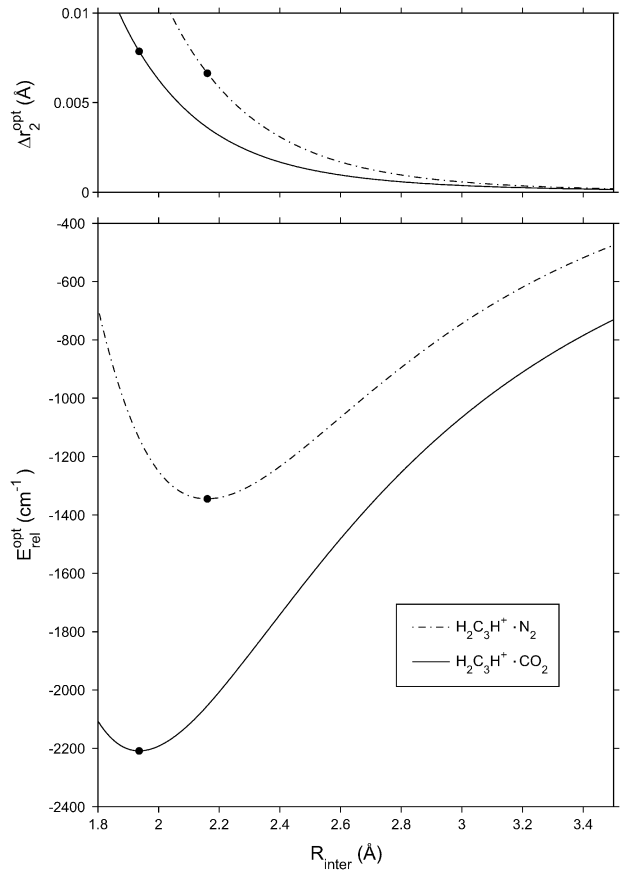

Fig. 7 Optimized relative energies and changes in H-bound CH distances as a function of the intermolecular separation for C_{2v} Min structures. Results obtained by CCSD(T*)-F12a with basis (T, Q).

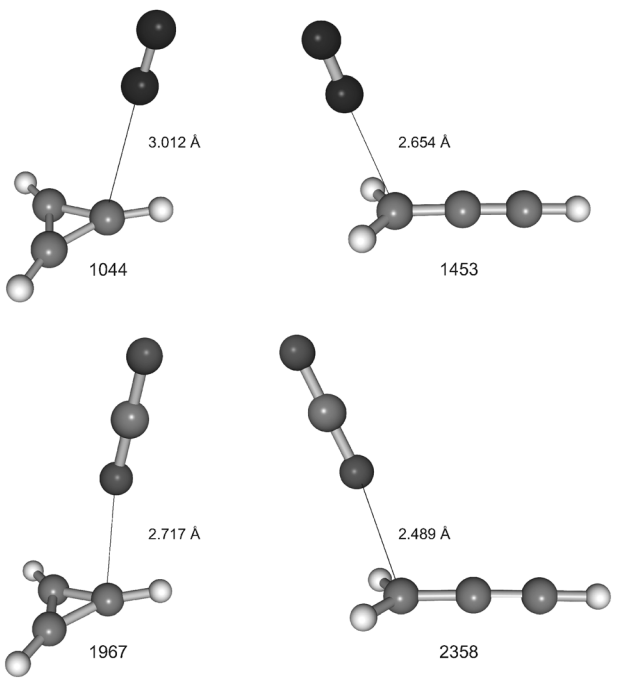

Fig. 8 C_s Min 1 equilibrium structures and equilibrium dissociation energies D_e (in cm^{-1}) for complexes with L = N_2 and CO_2. Results obtained by CCSD(T*)-F12a with basis (T, Q).

Table 4 Changes in intramolecular equilibrium geometrical parameters and D_e values for complexes c-$C_3H_3^+ \cdot$L (C_s Min 1)[a]

Geometrical parameter	c-$C_3H_3^+ \cdot$Ne	c-$C_3H_3^+ \cdot$Ar	c-$C_3H_3^+ \cdot N_2$	c-$C_3H_3^+ \cdot CO_2$
r_{1e}/Å	−0.00005	−0.00016	−0.00036	−0.00069
β_e/°	−0.01	−0.05	−0.06	−0.10
R_{1e}/Å	−0.00029	−0.00084	−0.00180	−0.00274
R_{2e}/Å	0.00001	0.00014	0.00017	−0.00018
r_{2e}/Å	−0.00018	−0.00046	−0.00143	−0.00194
R_{1e}^L			−0.00132	0.00992
R_{2e}^L				−0.00971
D_e/cm^{-1}	210.6	586.8	1043.7	1966.5

[a] CCSD(T*)-F12a; basis: (T, Q).

Table 5 Changes in intramolecular equilibrium geometrical parameters and D_e values for complexes $H_2C_3H^+ \cdot$L (C_s Min 1)[a]

Geometrical parameter	$H_2C_3H^+ \cdot$Ne	$H_2C_3H^+ \cdot$Ar	$H_2C_3H^+ \cdot N_2$	$H_2C_3H^+ \cdot CO_2$
R_{1e}/Å	−0.00012	−0.00056	−0.00148	−0.00193
α_e/°	−0.04	−0.13	−0.27	−0.25
R_{1e}/Å	−0.00035	−0.00208	−0.00424	−0.00423
R_{2e}/Å	−0.00030	−0.00156	−0.00325	−0.00368
r_{2e}/Å	−0.00007	−0.00051	−0.00098	−0.00131
R_{1e}^L			−0.00020	0.01065
R_{2e}^L				−0.01093
D_e/cm^{-1}	241.1	798.4	1452.6	2357.7

[a] CCSD(T*)-F12a; basis: (T, Q).

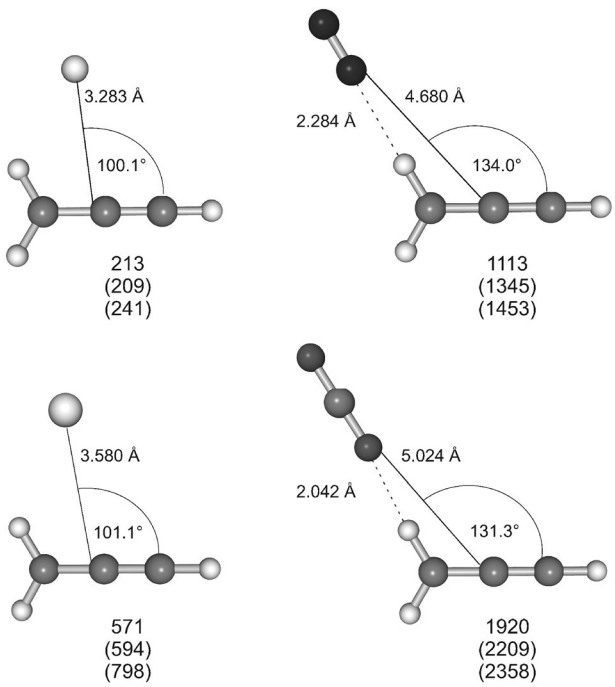

Fig. 9 Planar C_s equilibrium structures and equilibrium dissociation energies D_e (in cm^{-1}) for complexes with L = N_2 and CO_2. Results obtained by CCSD(T*)-F12a with basis (T, Q).

no clear bonding type is apparent. The more strongly bound species with L = N_2 and L = CO_2 are characterized by almost linear hydrogen bonds to one of the two equivalent methylenic H atoms.

Table 6 Equilibrium dissociation energies (in cm^{-1}) for $C_3H_3^+ \cdot N_2$: dependence on method and basis set[a]

		c-$C_3H_3^+ \cdot N_2$		$H_2C_3H^+ \cdot N_2$	
Method	Basis	C_s Min 1	C_{2v} Min	C_s Min 1	C_{2v} Min
SCF	(T, Q)	471.1	626.3	520.1	725.6
SCF	(Q, 5)	461.9	621.4	513.6	720.2
SCF + CABS-S	(T, Q)	462.6	622.6	514.8	721.6
SCF + CABS-S	(Q, 5)	461.7	620.8	513.3	719.2
CCSD(T)-F12a	(T, Q)	1041.7	1175.7	1449.7	1343.0
CCSD(T)-F12a	(Q, 5)	1037.2	1165.5	1440.7	1332.3
CCSD(T)-F12b	(T, Q)	1044.1	1179.7	1451.7	1347.4
CCSD(T)-F12b	(Q, 5)	1039.1	1168.5	1442.2	1335.7
CCSD(T*)-F12a	(T, Q)	1043.7	1177.2	1452.6	1344.8
CCSD(T*)-F12a	(Q, 5)	1038.3	1166.3	1442.3	1333.2
CCSD(T*)-F12b	(T, Q)	1046.1	1181.1	1454.6	1349.2
CCSD(T*)-F12b	(Q, 5)	1040.2	1169.3	1443.8	1336.6

[a] Equilibrium structures optimized at level CCSD(T*)-F12a/(T, Q) are used in all the underlying calculations.

The dependence of equilibrium dissociation energies for complexes with L = N_2 on method and basis set is shown in Table 6. The energetically most favourable structures C_s Min 1 and C_{2v} Min are considered. Besides the four variants of CCSD(T)-F12*x*, the SCF contributions and SCF + CABS singles contributions to the D_e values are listed. The CABS singles correction is still significant for the smaller (T, Q) basis set, but does not exceed 1.0 cm^{-1} for the (Q, 5) basis. The contributions to D_e obtained with the latter basis set should thus be very close to the Hartree–Fock limit. At the explicitly correlated coupled cluster level, increase of the basis set from (T, Q) to (Q, 5) lowers the D_e values by 4.5–12.6 cm^{-1}, *i.e.*, by only 1.0% or below. Scaling of the contributions of connected triple substitutions has a very small effect on the D_e values. Those are enlarged by up to 2.9 cm^{-1} for the (T, Q) basis set and by only 0.8–1.6 cm^{-1} for the (Q, 5) basis. The differences between F12 variants $x = a$ and $x = b$ are also quite small. For the smaller basis, the maximum difference among the four complex structures considered is only 4.4 cm^{-1} and a still smaller value of 3.4 cm^{-1} is obtained for the larger basis set.

Comparison with standard CCSD(T) is made for C_{2v} Min of $H_2C_3H^+ \cdot N_2$, where calculations with basis set combination (cc-pV*n*Z, aug-cc-pV*n*Z) up to $n = 6$ are still feasible with our computational resources. A series of calculations with n = T, Q, 5, and 6 has been carried out, considering the basis set superposition error by means of the familiar counterpoise procedure (CP) of Boys and Bernardi.[38] Fig. 10 displays CP corrected and uncorrected D_e values obtained by standard CCSD(T) with 4 different basis sets. CCSD(T*)-F12a/(T, Q) equilibrium structures were used in all of the individual calculations for complexes and fragments. The graphs connecting CP corrected data (straight lines) or CP uncorrected data (dashed lines) both show monotonic behaviour and appear to converge to a common limit of *ca.* 1331 cm^{-1}, the smoother corrected values from below and the uncorrected ones from above. The estimated limiting value is only slightly smaller (by less than 0.5%) than all the four values obtained by the CP uncorrected explicitly correlated coupled cluster variants with basis set (Q, 5). The much cheaper (T, Q) basis still provides values all of which overestimate the CCSD(T) limit estimate by no more than 1.4%.

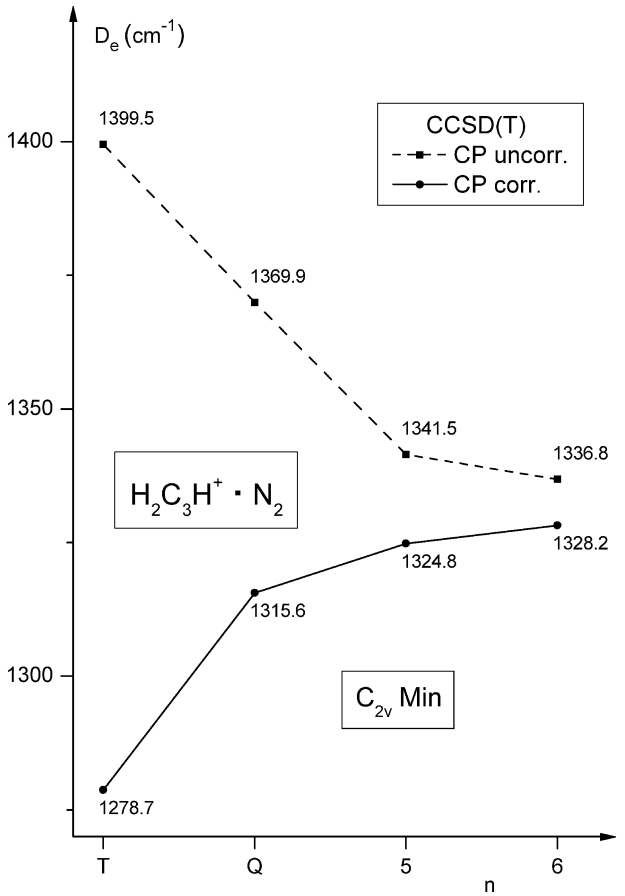

Fig. 10 Variation of the dissociation energy D_e with the size of the basis set in standard CCSD(T) calculations for $H_2C_3H^+ \cdot N_2$.

Equilibrium dissociation energies for complexes with L = CO_2 are listed in Table 7. On the whole, the situation is very similar as for L = N_2. Basis set differences are below 17 cm^{-1} and thus less than 1%, version $x = b$ yields slightly higher D_e values than version $x = a$ (less than 7 cm^{-1}) and the scaling of the connected triple substitutions produces even smaller changes (less than 1 cm^{-1}) than for the complexes with L = N_2.

Table 7 Equilibrium dissociation energies (in cm^{-1}) for $C_3H_3^+ \cdot CO_2$: dependence on method and basis set[a]

		c-$C_3H_3^+ \cdot CO_2$		$H_2C_3H^+ \cdot CO_2$	
Method	Basis	C_s Min 1	C_{2v} Min	C_s Min 1	C_{2v} Min
SCF	(T, Q)	1381.7	1606.9	1708.8	1785.3
SCF	(Q, 5)	1368.5	1601.2	1700.3	1779.1
SCF + CABS-S	(T, Q)	1370.0	1603.2	1702.1	1781.6
SCF + CABS-S	(Q, 5)	1362.8	1599.9	1699.4	1777.0
CCSD(T)-F12a	(T, Q)	1965.6	1998.4	2357.4	2208.9
CCSD(T)-F12a	(Q, 5)	1958.1	1984.1	2346.0	2194.4
CCSD(T)-F12b	(T, Q)	1969.8	2004.6	2361.0	2215.7
CCSD(T)-F12b	(Q, 5)	1961.6	1988.4	2348.9	2198.9
CCSD(T*)-F12a	(T, Q)	1966.5	1997.8	2357.7	2208.8
CCSD(T*)-F12a	(Q, 5)	1958.6	1983.9	2346.2	2194.5
CCSD(T*)-F12b	(T, Q)	1970.6	2003.9	2361.3	2215.6
CCSD(T*)-F12b	(Q, 5)	1962.1	1988.2	2349.1	2199.2

[a] Equilibrium structures optimized at level CCSD(T*)-F12a/(T, Q) are used in all the underlying calculations.

4. Calculated vibrational wavenumbers and (re)assignments of IRPD spectra

4.1 Results of explicitly correlated coupled cluster calculations

Harmonic vibrational wavenumbers have been calculated by CCSD(T*)-F12a and basis (T, Q) for three different structures of c-$C_3H_3^+$·Ne. The intramolecular wavenumbers are given in ESI† Table S14 along with data for the free cation. Upon complex formation, the symmetry is reduced from D_{3h} to C_{2v} or C_s and the doubly degenerate e' and e'' modes are split into two components. In the energetically lowest-lying structure (C_s Min 1), their separation is only 1.2 cm^{-1}, the lower component being blue-shifted with respect to free c-$C_3H_3^+$ by 1.1 cm^{-1}. Even smaller splittings and shifts are calculated for structures C_s Min 2 and C_{2v} Min.

CCSD(T*)-F12a intramolecular harmonic vibrational wavenumbers for four different structures of $H_2C_3H^+$·Ne are listed in ESI† Table S15 together with results for $H_2C_3H^+$. For the three structures of C_s symmetry, the calculated wavenumber shifts with respect to the bare cation are very small (2.0 cm^{-1} or less). A red-shift of 6.5 cm^{-1} is calculated for the acetylenic CH stretching vibration (ν_1) of C_{2v} Min and indicative of a very weak H-bond. In accordance with the slight reductions in all three CH bond lengths occurring upon complex formation, structure "C_s planar" experiences slight blue-shifts (0.4–1.3 cm^1) in all three CH stretching vibrations.

Results for C_s Min 1 and C_{2v} Min of c-$C_3H_3^+$·Ar are given in ESI† Table S16. No further minimum was found in full dimensionality. The minimum over (R, θ_1) space reported earlier[19] turned out to be a saddle point after complete geometry optimization and harmonic frequency analysis. For C_s Min 1, where the argon nucleus is closest to one of the equivalent carbon nuclei (R^e_{inter} = 3.264 Å), we predict blue-shifts in the CH stretching vibrations of 1.0–3.7 cm^{-1}. Structure C_{2v} Min is characterized by a splitting of the ν_4 mode of 20.1 cm^{-1} and a red-shift in the lower a_1 component of 19.6 cm^{-1}.

Results for $H_2C_3H^+$·Ar have been reported earlier.[20] ESI† Table S17 also includes data for structure C_s planar which was not studied before. Blue-shifts of 4.9–6.4 cm^{-1} are calculated for the CH stretching vibrations of the global minimum C_s Min 1, while a red-shift of 43.4 cm^{-1} is obtained for ν_1 (C_{2v} Min). Very small shifts (−0.8 to 1.8 cm^{-1}) are predicted for the local minimum C_s planar, thus exhibiting no sign of H-bonding.

Harmonic wavenumber calculations for c-$C_3H_3^+$·N_2 have been restricted to C_{2v} Min and C_s Min 1. CCSD(T*)-F12a/(T, Q) results for the former, which corresponds to the lowest energy minimum found, are reported in Table 8 along with previous MP2 values.[10] While MP2 performs poorly for the N_2 ligand, the results for c-$C_3H_3^+$ are reasonably good, the largest deviation from the present coupled cluster calculations not exceeding 50 cm^{-1}. For the asymmetric CH stretching vibration ν_4, the splitting is calculated to be 47.0 cm^{-1}, to be compared with the previous MP2 value of 62 cm^{-1}.[10] With respect to free c-$C_3H_3^+$, the lower component of a_1 symmetry is red-shifted by −45.3 cm^{-1}. Combining the neon matrix value for c-$C_3H_3^+$[17] with the shifts from the present work, we calculate the two ν_4 components at 3085 cm^{-1} (a_1) and 3132 cm^{-1} (b_2).

Table 8 Calculated harmonic wavenumbers and shifts (in cm^{-1}) for intramolecular vibrations of c-$C_3H_3^+$·N_2 (C_{2v} Min)

Vibration	CCSD(T*)-F12a[a]	MP2 (full)[b]
ω_1 (a_1)	3295.5 (−7.1)	3344 (−8)
ω_2 (a_1)	3210.7 (−45.3)	3243 (−59)
ω_3 (a_1)	1639.9 (−1.9)	1653 (−4)
ω_4 (a_1)	1320.2 (+1.4)	1340 (1)
ω_5 (a_1)	942.9 (−0.3)	952 (−1)
ω_6 (a_2)	1016.6 (+0.2)	1032 (0)
ω_7 (b_1)	1041.6 (+25.2)	1075 (18)
ω_8 (b_1)	776.3 (+15.1)	806 (22)
ω_9 (b_2)	3257.8 (+1.7)	3305 (3)
ω_{10} (b_2)	1314.2 (−4.6)	1333 (−6)
ω_{11} (b_2)	1063.9 (+13.5)	1079 (47)
ω_{12} (b_2)	965.4 (+22.1)	982 (29)
ω_{N_2} (a_1)	2364.3 (+4.7)	2208 (4)

[a] Basis: (T, Q). [b] Ref. 10. Basis: 6-311G (2df, 2pd).

Within the familiar double harmonic approximation, the molar absorption intensity of the former is calculated to be 298 km mol^{-1}, 1.5 times larger than the corresponding value for the doubly degenerate vibration of free c-$C_3H_3^+$. We thus expect a strong signal of c-$C_3H_3^+$·N_2 in the IRPD spectrum close to 3085 cm^{-1}. According to the present calculations, the other IR active vibration of the cyclopropenyl cation (ν_5 of e'' symmetry) is split by 25.0 cm^{-1} (difference between ω_7 and ω_6 of Table 8), the upper b_1 component experiencing a blue-shift of 25.2 cm^{-1}.

Owing to its significantly higher energy and for economical reasons, harmonic wavenumbers of C_s Min 1 (c-$C_3H_3^+$·N_2) have only been calculated with the small (D, T) basis set. For the three CH stretching vibrations, the CCSD(T*)-F12a method yields (in cm^{-1}) 3310.1 (+7.5), 3266.3 (+10.2), and 3258.4 (+2.3), where the small shifts with respect to free c-$C_3H_3^+$ are given in parentheses.

Table 9 lists CCSD(T*)-F12a harmonic wavenumbers and shifts for intramolecular vibrations of c-$C_3H_3^+$·CO_2 in its C_{2v} Min and C_s Min 1 structures. For the former, the splitting of the ν_4 band is calculated to be 50.6 cm^{-1} and the red-shift of the lower a_1 component amounts to 47.1 cm^{-1}.

Table 9 CCSD(T*)-F12a harmonic wavenumbers and shifts (in cm^{-1}) for intramolecular vibrations of c-$C_3H_3^+$·CO_2 (C_{2v} Min and C_s Min 1)

Vibration[a]		C_{2v} Min[b]	C_s Min 1[c]
c-$C_3H_3^+$	1	3297.3 (−5.3)	3315.1 (+13.4)
	2	3259.6 (+3.5)	3271.7 (+16.8)
	3	3209.0 (−47.1)	3262.2 (+7.3)
	4	1636.7 (−5.1)	1642.3 (+6.1)
	5	1320.4 (+1.6)	1320.3 (+5.0)
	6	1309.9 (−8.9)	1317.3 (+2.0)
	7	1063.7 (+13.3)	1051.6 (+2.5)
	8	1042.9 (+26.5)	1012.3 (−3.2)
	9	1016.6 (+0.2)	1005.0 (−10.5)
	10	965.2 (+21.9)	945.9 (+3.0)
	11	943.5 (+0.2)	944.5 (+1.6)
	12	774.5 (+13.3)	756.7 (+1.4)
CO_2	1	2401.5 (+8.2)	2395.2 (+7.9)
	2	1353.1 (+1.1)	1347.8 (+0.5)
	3	663.1 (−9.8)	665.3 (−5.9)
	4	663.1 (−9.8)	664.6 (−6.6)

[a] Vibrations are numbered individually for c-$C_3H_3^+$ and CO_2 according to decreasing wavenumber. [b] Basis: (T, Q). [c] Basis: (D, T).

Table 10 CCSD(T*)-F12a cation vibrational wavenumbers (in cm^{-1}) for $H_2C_3H^+$·L (lowest C_s structure)[a]

Vibration[b]	$H_2C_3H^+$·Ne[c]	$H_2C_3H^+$·Ar[c]	$H_2C_3H^+$·N_2[d]	$H_2C_3H^+$·CO_2[d]
ν_1 (a_1)	3237 (+1)	3241 (+5)	3247 (+11)	3249 (+13)
ν_2 (a_1)	2992 (+2)	2996 (+6)	3006 (+16)	3011 (+21)
ν_3 (a_1)	2080 (0)	2081 (+1)	2083 (+3)	2084 (+4)
ν_4 (a_1)	1446 (0)	1446 (0)	1449 (+3)	1448 (+2)
ν_5 (a_1)	1123 (0)	1119 (−4)	1119 (−4)	1119 (−4)
ν_6 (b_1)	1100 (+1)	1097 (−2)	1098 (−1)	1098 (−1)
ν_7 (b_1)	873 (+1)	867 (−5)	864 (−8)	862 (−10)
ν_8 (b_1)	264 (0)	281 (+17)	285 (+21)	283 (+19)
ν_9 (b_2)	3082 (+2)	3086 (+6)	3097 (+17)	3101 (+21)
ν_{10} (b_2)	1017 (0)	1017 (0)	1019 (+2)	1019 (+2)
ν_{11} (b_2)	615 (0)	618 (+3)	624 (+9)	621 (+6)
ν_{12} (b_2)	301 (+3)	302 (+4)	307 (+9)	303 (+5)

[a] Obtained by summing up results from VCI calculations for free $H_2C_3H^+$ and harmonic shifts arising from complex formation (in parentheses). [b] Assignment for free $H_2C_3H^+$ is employed. [c] Basis (T, Q) is used in the calculation of wavenumber shifts. [d] Basis (D, T) is used in the calculation of wavenumber shifts.

Table 12 CCSD(T*)-F12a cation vibrational wavenumbers (in cm^{-1}) for $H_2C_3H^+$·L (planar C_s structure)[a]

Vibration[b]	$H_2C_3H^+$·Ne[c]	$H_2C_3H^+$·Ar[c]	$H_2C_3H^+$·N_2[d]	$H_2C_3H^+$·CO_2[d]
ν_1 (a_1)	3236 (0)	3238 (+2)	3241 (+5)	3243 (+7)
ν_2 (a_1)	2991 (+1)	2989 (−1)	2969 (−21)	2970 (−20)
ν_3 (a_1)	2080 (0)	2080 (0)	2079 (−1)	2078 (−2)
ν_4 (a_1)	1447 (+1)	1441 (−5)	1454 (+8)	1453 (+7)
ν_5 (a_1)	1123 (0)	1122 (−1)	1124 (+1)	1127 (+4)
ν_6 (b_1)	1100 (+1)	1102 (+3)	1118 (+19)	1116 (+17)
ν_7 (b_1)	872 (0)	871 (−1)	871 (−1)	870 (−2)
ν_8 (b_1)	264 (0)	264 (0)	278 (+14)	274 (+10)
ν_9 (b_2)	3081 (+1)	3080 (0)	3065 (−15)	3067 (−13)
ν_{10} (b_2)	1015 (−2)	1019 (+2)	1028 (+11)	1027 (+10)
ν_{11} (b_2)	614 (−1)	612 (−3)	611 (−4)	610 (−5)
ν_{12} (b_2)	300 (+2)	298 (0)	308 (+10)	308 (+10)

[a] Obtained by summing up results from VCI calculations for free $H_2C_3H^+$ and harmonic shifts arising from complex formation (in parentheses). [b] Assignment for free $H_2C_3H^+$ is employed. [c] Basis (T, Q) is used in the calculation of wavenumber shifts. [d] Basis (D, T) is used in the calculation of wavenumber shifts.

Both values are only slightly larger than for c-$C_3H_3^+$·N_2. In the same way as for that species, we calculate the a_1 component of ν_4 (c-$C_3H_3^+$·CO_2) at 3083 cm^{-1} and the b_2 component at 3134 cm^{-1}. For the former, a large intensity of 410 km mol^{-1} is predicted. The energetically less favourable structure C_s Min 1 is characterized by blue-shifts (7.3–16.8 cm^{-1}) in the CH stretching vibrations. The splitting in the ν_4 mode is predicted as 9.5 cm^{-1}.

Predictions for the cation wavenumbers of complexes of type $H_2C_3H^+$·L (L = Ne, Ar, N_2, and CO_2) are obtained by combining the results of the previous VCI calculations[20] with harmonic shifts from the present work. Tables 10–12 list the predicted wavenumbers along with the shifts for three different structures. Data for the most stable structure C_s Min 1 are collected in Table 10. Along the series of ligands, ordered by increasing D_e value, clear trends are discernible. All the three CH stretching vibrations (ν_1, ν_2, and ν_9) exhibit blue-shifts ranging from 1 cm^{-1} (L = Ne) up to 21 cm^{-1} (L = CO_2). The vibrations in the range between 1000 and 2100 cm^{-1} are only slightly affected by complex formation and show shifts of less than 5 cm^{-1}. Larger shifts of up to 21 cm^{-1} are calculated for the ν_8 vibration which, owing to its low wavenumber, is not accessible to current IRPD spectroscopy.

Table 11 CCSD(T*)-F12a cation vibrational wavenumbers (in cm^{-1}) for $H_2C_3H^+$·L (H-bound C_{2v} Min)[a]

Vibration[b]	$H_2C_3H^+$·Ne	$H_2C_3H^+$·Ar	$H_2C_3H^+$·N_2	$H_2C_3H^+$·CO_2
ν_1 (a_1)	3229 (−7)	3193 (−43)	3141 (−95)	3128 (−108)
ν_2 (a_1)	2990 (0)	2991 (+1)	2992 (+2)	2994 (+4)
ν_3 (a_1)	2079 (−1)	2075 (−5)	2070 (−10)	2069 (−11)
ν_4 (a_1)	1446 (0)	1447 (+1)	1447 (+1)	1448 (+2)
ν_5 (a_1)	1124 (+1)	1125 (+2)	1126 (+3)	1128 (+5)
ν_6 (b_1)	1098 (−1)	1098 (−1)	1096 (−3)	1094 (−5)
ν_7 (b_1)	878 (+6)	894 (+22)	929 (+57)	928 (+56)
ν_8 (b_1)	266 (+2)	268 (+4)	281 (+17)	276 (+12)
ν_9 (b_2)	3080 (0)	3080 (0)	3081 (+1)	3083 (+2)
ν_{10} (b_2)	1017 (0)	1018 (+1)	1018 (+1)	1019 (+2)
ν_{11} (b_2)	625 (+10)	649 (+34)	701 (+86)	697 (+82)
ν_{12} (b_2)	299 (+1)	300 (+2)	301 (+3)	300 (+2)

[a] Obtained by summing up results from VCI calculations for free $H_2C_3H^+$ and harmonic shifts arising from complex formation (in parentheses). Basis (T, Q) is used in the CCSD(T*)-F12a calculations. [b] Assignment for free $H_2C_3H^+$ is employed.

The H-bound species of C_{2v} symmetry (see Table 11) show characteristic red-shifts in the acetylenic stretching vibration ν_1, ranging from 7 cm^{-1} for very weakly bound $H_2C_3H^+$·Ne up to 108 cm^{-1} for $H_2C_3H^+$·CO_2. On the other hand, and also typical for H-bonded complexes with acetylenic groups,[39–41] the CCH bending vibrations ν_7 and ν_{11} experience blue-shifts of up to 86 cm^{-1}. The IR intensities of the ν_1 bands increase strongly in the series L = Ne–CO_2. Their calculated values (in km mol^{-1}) are 163, 290, 400, and 600.

Finally, Table 12 predicts cation wavenumbers for the planar C_s minima of $H_2C_3H^+$·L complexes. For $H_2C_3H^+$·Ne and $H_2C_3H^+$·Ar, the shifts in the CH stretching vibrations are very small. This is in line with the corresponding equilibrium structures (see Fig. 9), which show no H-bonding character. As expected for complexes with a methylenic H-bond, the planar C_s structures for $H_2C_3H^+$·N_2 and $H_2C_3H^+$·CO_2 show red-shifts in the methylenic CH stretching vibrations ν_2 and ν_9. Like for the most stable structures C_s Min 1, the acetylenic stretching vibrations are predicted to exhibit small blue-shifts.

4.2 (Re)assignments of IRPD spectra

Fig. 11 shows IRPD spectra of $C_3H_3^+$·L complexes (L = Ne, Ar, O_2, N_2, and CO_2) in the C–H stretching range recorded in the $C_3H_3^+$ fragment channel. It is a revised version of Fig. 3 from ref. 12, with the arrow designating ν_1 ($H_2C_3H^+$) having been moved to the correct position (from 3319 to 3236 cm^{-1}). Positions and widths of the individual bands along with proposed (re)assignments are given in Table 13. We will discuss the spectra of Fig. 11 from the bottom, starting with L = Ne. The broad band around 3130 cm^{-1} is readily assigned to ν_4 (c-$C_3H_3^+$·Ne). Owing to the small energetic separations of three different structures (D_e values ranging from 183 to 209 cm^{-1}, Table 1) and minor shifts and splittings upon complexation, all of them may contribute to that band. The band at 3184 cm^{-1} is probably due to the combination tone ν_3 + ν_5 of

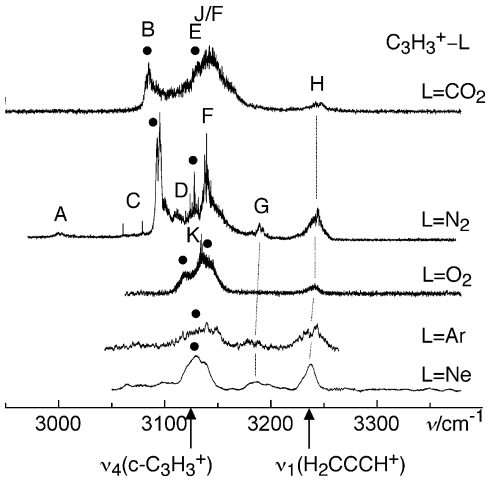

Fig. 11 IRPD spectra of $C_3H_3^+$·L dimers with L = Ne, Ar, O_2, N_2, and CO_2 recorded in the $C_3H_3^+$ fragment channel (adapted from ref. 12). The observed transitions and their suggested vibrational and isomer assignments are listed in Table 13. The arrows below the wavenumber scale indicate the positions of ν_4 of c-$C_3H_3^+$ (3125 ± 4 cm^{-1}) and of the CCSD(T*)-F12a value for ν_1 of $H_2C_3H^+$ (3236 cm^{-1}).

$H_2C_3H^+$·Ne, which was predicted for the free cation to occur at 3185 cm^{-1} (Table 4 of ref. 20). According to Table 10, the acetylenic stretching vibration ν_1 for C_s Min 1 of $H_2C_3H^+$·Ne is calculated at 3237 cm^{-1}. This structure is expected to dominate the band at 3238 cm^{-1} but the energetically less favourable structures C_{2v} Min, C_s Min 2, and planar C_s Min may contribute as well.

The IRPD spectra of $C_3H_3^+$·Ar[12,18] have been discussed in detail in our previous work,[20] including a very critical examination of the IRPD spectra of Ricks *et al.*[18] We are convinced that the broad band around 3136 cm^{-1} results from ν_4 (c-$C_3H_3^+$·Ar); different isomeric structures of this complex may contribute. For $H_2C_3H^+$·Ar, the C-bound C_s Min 1 was calculated to have a significantly higher D_e value than all the other local minima. This structure should thus have the highest population in the molecular beam and dominate the IRPD spectrum shown in Fig. 11. Consequently, we assign the band at 3182 cm^{-1} to $\nu_3 + \nu_5$ and the band at 3239 cm^{-1} to ν_1 of C-bound $H_2C_3H^+$·Ar.

Little progress has been made in the assignment of the IRPD spectrum for $C_3H_3^+$·O_2. The band at 3240 cm^{-1} may safely be assigned to an essentially free acetylenic stretching vibration of $H_2C_3H^+$·O_2 (ν_1). This band is quite weak and the only one attributable to complexes of the propargyl cation. The previous assignments of the three observed bands B, E, and K to c-$C_3H_3^+$·O_2 are currently left unchanged. On the basis of its rotational structure, band K was assigned to the degenerate ν_4 fundamental of a π-bonded c-$C_3H_3^+$·O_2 complex with C_{3v} symmetry, consistent with the flat PES presented in Fig. 5. Bands B and E were tentatively attributed to the a_1 and b_2 components of ν_4 of an H-bonded c-$C_3H_3^+$·O_2 complex. This assignment must, however, be questioned when considering the potential scan presented in Fig. 5, which does not exhibit a pronounced minimum at the H-bonded configuration. Clearly, firm characterization of the PESs and vibrational spectra of the isomeric $C_3H_3^+$·O_2 complexes requires additional experimental and theoretical studies.

The IRPD spectrum for $C_3H_3^+$·N_2 is quite rich in structure. The calculations predict that the equilibrium dissociation energies of the two $H_2C_3H^+$·N_2 isomers C_s Min 1 (C-bound) and C_{2v} Min (H-bound) are close to each other (D_e = 1442 and 1333 cm^{-1}, Table 6). Similarly, the binding energies of the two c-$C_3H_3^+$·N_2 isomers C_s Min 1 (C-bound) and

Table 13 Positions and widths (fwhm, in parentheses) of the observed transitions in the IRPD spectra of $C_3H_3^+$–L (Fig. 11), along with the new suggested isomer and vibrational assignment

L	Position/cm^{-1}	Transition	Structure of complex	Vibration
Ne	3130 (24)	B/E	c-$C_3H_3^+$·Ne	ν_4
	3184 (17)	G	H_2CCCH^+·Ne	$\nu_3 + \nu_5$
	3238 (11)	H	H_2CCCH^+·Ne	ν_1
Ar	3136 (39)	B/E	c-$C_3H_3^+$·Ar	ν_4
	3182 (15)	G	C-bound H_2CCCH^+·Ar	$\nu_3 + \nu_5$
	3239 (27)	H	C-bound H_2CCCH^+·Ar	ν_1
O_2	3118 (8)	B	H-bound c-$C_3H_3^+$·O_2?	$\nu_4(1)$?
	3140 (19)	E	H-bound c-$C_3H_3^+$·O_2?	$\nu_4(2)$?
	3240 (10)	H	C-bound H_2CCCH^+·O_2	ν_1
	3133.03[a]	K	π-bound c-$C_3H_3^+$·O_2	$\nu_4(e)$
N_2	3001 (6)	A	H-bound H_2CCCH^+·N_2	ν_2
	3013 (5)[b]	A	C-bound H_2CCCH^+·N_2	ν_2
	3094 (5)	B	H-bound c-$C_3H_3^+$·N_2	$\nu_4(a_1)$
	3104.91[a]	C	H-bound H_2CCCH^+·N_2	$\nu_3 + \nu_{10}$
	3113 (10)	D	C-bound H_2CCCH^+·N_2	$\nu_3 + \nu_{10}$
	3128.75[a]	E	H-bound c-$C_3H_3^+$·N_2	$\nu_4(b_2)$
	3139 (4)	F	H-bound H_2CCCH^+·N_2	ν_1
	3191 (6)	G	C/H-bound H_2CCCH^+·N_2	$\nu_3 + \nu_5$
	3243 (13)	H	C-bound H_2CCCH^+·N_2	ν_1
CO_2	3084 (10)	B	H-bound c-$C_3H_3^+$·CO_2	$\nu_4(a_1)$
	3130.03[a]	E	H-bound c-$C_3H_3^+$·CO_2	$\nu_4(b_2)$
	3142 (31)	J	C-bound c-$C_3H_3^+$·CO_2	$\nu_4(a'',a')$
	3142 (31)	F	H-bound H_2CCCH^+·CO_2	ν_1
	3245 (12)	H	C-bound H_2CCCH^+·CO_2	ν_1

[a] Fitted band origin. [b] Shoulder.

C_{2v} Min (H-bound) are not very different (D_e = 1038 and 1166 cm^{-1}). Therefore, we may expect that all four isomers are populated in the molecular beam. The interpretation of the experimental spectrum is compatible with this scenario, although no clear-cut evidence for the presence of C-bound c-$C_3H_3^+ \cdot N_2$ is evident. The two perpendicular bands C and E exhibit resolved K structure and unambiguously prove the presence of two isomers, namely the H-bound isomers of $H_2C_3H^+ \cdot N_2$ and c-$C_3H_3^+ \cdot N_2$. Band H at 3243 cm^{-1} is reassigned to the free ν_1 fundamental of C-bound $H_2C_3H^+ \cdot N_2$ predicted at 3247 cm^{-1} and clearly verifies the presence of this isomer in the molecular beam. Band F at 3139 cm^{-1} is attributed to the ν_1 fundamental of the H-bonded $H_2C_3H^+ \cdot N_2$ isomer, in excellent agreement with the predicted wavenumber of 3141 cm^{-1}, which implies a red-shift of 95 cm^{-1} for this proton donor stretching mode upon H-bonding. The tail to the blue of band F is a typical IR spectroscopic signature of a proton-donor stretching vibration[4] and provides further evidence for the given vibrational and isomer assignment. From the experimental intensity ratio of bands F and H ($\sim$2), we can roughly estimate the population ratio for both isomers by taking into account that the calculated IR oscillator strength increases by a factor of $\sim$4 upon formation of the H-bond. The obtained population ratio of 2 : 1 for C-bound *versus* H-bound $H_2C_3H^+ \cdot N_2$ is consistent with their roughly similar binding energies and the fact that there are two non-equivalent C-bound minima on the $H_2C_3H^+ \cdot N_2$ PES, whereas there is only a single H-bound minimum. Band G at 3191 cm^{-1} is assigned to the combination band $\nu_3 + \nu_5$ of both H-bound and C-bound $H_2C_3H^+ \cdot N_2$. Bands B and E at 3094 and 3129 cm^{-1} were interpreted as the parallel (a_1) and perpendicular (b_2) components of ν_4 of H-bonded c-$C_3H_3^+ \cdot N_2$. The partly-resolved rotational structure of band E proves that H-bonded c-$C_3H_3^+ \cdot N_2$ is present in the beam and that it has indeed C_{2v} symmetry. The experimental splitting of 35 cm^{-1} between the a_1 and b_2 components of ν_4 agrees reasonably well with the predicted value (47 cm^{-1}). The perpendicular transition C with band origin at 3105 cm^{-1} was unambiguously assigned to H-bonded $H_2C_3H^+ \cdot N_2$ on the basis of its rotational structure. Analysis of the latter confirms that this isomer has indeed a geometry with C_{2v} symmetry and a linear C–C–C–H $\cdots$ N–N backbone, as predicted by the calculations. Inspection of Table 12 immediately suggests an assignment of band C to the combination tone $\nu_3 + \nu_{10}$, whose frequency can be estimated as 2070 + 1018 = 3088 cm^{-1} from the sum of the individual fundamentals of this isomer. The ν_3 fundamental has high predicted IR intensity and the $\nu_3 + \nu_{10}$ combination is the only binary one with correct symmetry (b_2) and wavenumber. Band D at 3113 cm^{-1} is tentatively assigned to $\nu_3 + \nu_{10}$ of the C-bonded $H_2C_3H^+ \cdot N_2$ isomer. The measured small blue-shift with respect to the corresponding vibration of the H-bonded isomer of +8 cm^{-1} is consistent with the predicted shift of +14 cm^{-1}. Band A at 3001 cm^{-1} was initially assigned to $2\nu_4$ of a $H_2C_3H^+ \cdot N_2$ complex.[11] This assignment is now rejected, as ν_4 is predicted near 1450 cm^{-1} with negligible complexation shift. Anharmonic calculations predict for the $2\nu_4$ overtone of isolated $H_2C_3H^+$ a wavenumber (2866 cm^{-1}) far away from the position of band A and also low IR activity (3.6 km mol^{-1}).[20] Thus, we switch the assignment to ν_2 of $H_2C_3H^+ \cdot N_2$. The calculations predict ν_2 = 2990 cm^{-1} for $H_2C_3H^+$ with significantly higher IR intensity (25 km mol^{-1}). Closer inspection of the band A at 3001 cm^{-1} reveals a weaker shoulder at 3013 cm^{-1}. These two components are now attributed to ν_2 of H-bound and C-bound $H_2C_3H^+ \cdot N_2$, compatible with the predicted wavenumbers of 2992 and 3006 cm^{-1}, respectively.

Interestingly, the IRPD spectrum of $C_3H_3^+ \cdot CO_2$ is simpler than the one of $C_3H_3^+ \cdot N_2$ and closer in appearance to the one of $C_3H_3^+ \cdot O_2$. The present calculations yield quite similar equilibrium dissociation energies for the C-bound and H-bound $H_2C_3H^+ \cdot CO_2$ isomers, with D_e = 2346 and 2195 cm^{-1} (Table 7). Also the C-bound and H-bound isomers of c-$C_3H_3^+ \cdot CO_2$ are very close in energy, D_e = 1959 and 1984 cm^{-1}. Therefore, we may expect significant population of all four isomers in the molecular beam expansion. The bands B and E at 3084 and 3130 cm^{-1} were assigned to the a_1 and b_2 components of ν_4 of H-bonded c-$C_3H_3^+ \cdot CO_2$. The measured splitting of 46 cm^{-1} agrees well with the calculated value (51 cm^{-1}). The rotational structure of band E proves that H-bonded c-$C_3H_3^+ \cdot CO_2$ is present in the molecular beam expansion and that this isomer has a geometry with C_{2v} symmetry as predicted by the calculations. Band H at 3245 cm^{-1} is reassigned to ν_1 of C-bonded $H_2C_3H^+ \cdot CO_2$, in excellent agreement with the calculated wavenumber of 3247 cm^{-1}. The detection of the free acetylenic C–H stretching band verifies the presence of this particular isomer in the molecular beam. The intensity of this band is quite weak, suggesting only small population of C-bonded $H_2C_3H^+ \cdot CO_2$. As this isomer is calculated as the global minimum of the $H_2C_3H^+ \cdot CO_2$ PES, the population of the less stable H-bonded $H_2C_3H^+ \cdot CO_2$ is even smaller. The low concentration of $H_2C_3H^+$ in the CO_2 expansion explains also the absence of bands C and G in the IRPD spectrum of $H_2C_3H^+ \cdot CO_2$. The broad transition at 3142 cm^{-1} with a large width of 31 cm^{-1} is tentatively assigned to the two unresolved ν_4 components of C-bonded $H_2C_3H^+ \cdot CO_2$ (band J) and/or ν_1 of H-bonded $H_2C_3H^+ \cdot CO_2$ (band F). The latter assignment is consistent with the calculated wavenumber of 3141 cm^{-1}.

The following two general trends along the $H_2C_3H^+ \cdot L$ and c-$C_3H_3^+ \cdot L$ series predicted by the calculations are confirmed by the experimental spectra. Firstly, band H is newly attributed to ν_1 of the C-bound $H_2C_3H^+ \cdot L$ dimers. The CCSD(T*)-F12a value for the free cation is 3236 cm^{-1} and the harmonic frequency blue-shifts upon complexation increase systematically from Ne (+1 cm^{-1}) to CO_2 (+13 cm^{-1}). This observation is in nice agreement with the experimental trend, with slightly smaller blue-shifts (+7 cm^{-1} between Ne and CO_2). Secondly, the ν_4 of splitting of H-bonded c-$C_3H_3^+ \cdot L$ is predicted to increase monotonically with the interaction strength from Ne to CO_2, again in line with the experimental trend.

5. Conclusions

Explicitly correlated coupled cluster theory has been employed to study 1 : 1 complexes of the fundamental cations c-$C_3H_3^+$ and $H_2C_3H^+$ with Ne, Ar, N_2, and CO_2 close to the AO basis set limit. Thereby, accurate data could be established for equilibrium structures and equilibrium dissociation energies D_e. The determination of accurate D_0 values, which refer to

the vibrational ground states, remains a difficult problem since anharmonicity effects on the intermolecular vibrations may be large and their reliable treatment is outside of the scope of the present work. For the calculation of shifts in the intramolecular vibrations of the cations, which are of primary interest to the present work, the harmonic approximation appears to be sufficient for the complexes studied here. The high accuracy of the predicted wavenumbers enables a reliable and significantly refined assignment of the previously reported IRPD spectra. Throughout, the C-bonds in $H_2C_3H^+$·L have larger D_e values than the acetylenic H-bonds, which in turn are significantly stronger than the H-bonds to the methylenic protons. In the case of the c-$C_3H_3^+$·L dimers, the H-bonds to the aromatic CH protons are also of similar energy as the intermolecular C-bonds. In general, the interaction of the ligands with $H_2C_3H^+$ is stronger than with c-$C_3H_3^+$. In contrast to complexes with Ne, Ar, N_2, and CO_2, accurate calculations with the open-shell O_2 ligand are more challenging and should be the target of future efforts.

Acknowledgements

This study was supported by the Deutsche Forschungsgemeinschaft (DO 729/3) and the Fonds der Chemischen Industrie.

References

1 J. R. Roscioli, L. R. McCunn and M. A. Johnson, *Science*, 2007, **316**, 249–254.
2 G. Zundel, in *The Hydrogen Bond-Recent Developments in Theory and Experiments. II Structure and Spectroscopy*, ed. P. Schuster, G. Zundel and C. Sandorfy, North-Holland, Amsterdam, 1976.
3 X. Huang, B. J. Braams and J. M. Bowman, *J. Chem. Phys.*, 2005, **122**, 044308.
4 E. J. Bieske and O. Dopfer, *Chem. Rev.*, 2000, **100**, 3963.
5 O. Dopfer, *Int. Rev. Phys. Chem.*, 2003, **22**, 437.
6 M. A. Duncan, *Int. J. Mass Spectrom.*, 2000, **200**, 545.
7 *Carbocation Chemistry*, ed. G. K. Prakash and G. A. Olah, Wiley, New York, 2004.
8 P. Goldberg, J. A. Hopkinson, A. Mathias and A. E. Williams, *Org. Mass Spectrom.*, 1970, **3**, 1009.
9 F. P. Lossing, *Can. J. Chem.*, 1972, **50**, 3973.
10 O. Dopfer, D. Roth and J. P. Maier, *J. Am. Chem. Soc.*, 2002, **124**, 494.
11 O. Dopfer, D. Roth and J. P. Maier, *Int. J. Mass Spectrom.*, 2002, **218**, 281.
12 D. Roth and O. Dopfer, *Phys. Chem. Chem. Phys.*, 2002, **4**, 4855–4865.
13 D. W. Minsek and P. Chen, *J. Phys. Chem.*, 1990, **95**, 8399.
14 P. Botschwina, M. Horn, J. Flügge and S. Seeger, *J. Chem. Soc., Faraday Trans.*, 1993, **89**, 2219.
15 T. Gilbert, R. Pfab, I. Fischer and P. Chen, *J. Chem. Phys.*, 2000, **112**, 2575.
16 P. Chen, I. Fischer and R. Pfab, *J. Chem. Phys.*, 2009, **131**, 159904.
17 M. Wyss, E. Riaplov and J. P. Maier, *J. Chem. Phys.*, 2001, **114**, 10355.
18 A. M. Ricks, G. E. Douberly, P. v. R. Schleyer and M. A. Duncan, *J. Chem. Phys.*, 2010, **132**, 051101.
19 P. Botschwina and R. Oswald, *J. Chem. Phys.*, 2011, **134**, 044305.
20 P. Botschwina, R. Oswald and G. Rauhut, *Phys. Chem. Chem. Phys.*, 2011, **13**, 7921.
21 T. B. Adler, G. Knizia and H.-J. Werner, *J. Chem. Phys.*, 2007, **127**, 221106.
22 G. Knizia, T. B. Adler and H.-J. Werner, *J. Chem. Phys.*, 2009, **130**, 054104.
23 H.-J. Werner, G. Knizia, T. B. Adler and O. Marchetti, *Z. Phys. Chem.*, 2010, **224**, 493.
24 H.-J. Werner, T. B. Adler, G. Knizia and F. R. Manby, *Recent Progress in Coupled Cluster Methods: Theory and Applications*, ed. P. Carsky, J. Pittner and J. Paldus, Springer, 2010.
25 K. Raghavachari, G. W. Trucks, J. A. Pople and M. Head-Gordon, *Chem. Phys. Lett.*, 1989, **157**, 479.
26 D. P. Tew, C. Hättig, R. A. Bachorz and W. Klopper, *Recent Progress in Coupled Cluster Methods: Theory and Applications*, ed. P. Carsky, J. Pittner and J. Paldus, Springer, 2010.
27 K. A. Peterson, T. B. Adler and H.-J. Werner, *J. Chem. Phys.*, 2008, **128**, 084102.
28 H. J. Werner and W. Meyer, *Mol. Phys.*, 1976, **31**, 855.
29 T. H. Dunning, Jr., *J. Chem. Phys.*, 1989, **90**, 1007.
30 R. A. Kendall, T. H. Dunning and R. J. Harrison, *J. Chem. Phys.*, 1992, **96**, 6796.
31 T. H. Dunning, Jr., K. A. Peterson and A. K. Wilson, *J. Chem. Phys.*, 2001, **114**, 9244 and references therein.
32 K. E. Yousaf and K. A. Peterson, *J. Chem. Phys.*, 2008, **129**, 184108.
33 K. E. Yousaf and K. A. Peterson, *Chem. Phys. Lett.*, 2009, **476**, 303.
34 F. Weigend, A. Köhn and C. Hättig, *J. Chem. Phys.*, 2002, **116**, 3175.
35 F. Weigend, *Phys. Chem. Chem. Phys.*, 2002, **4**, 4285.
36 C. Hättig, *Phys. Chem. Chem. Phys.*, 2005, **7**, 59.
37 H.-J. Werner, P. J. Knowles, R. Lindh, F. R. Manby and M. Schütz, et al., *MOLPRO version 2009.1, a package of ab initio programs*, 2009, see http://www.molpro.net.
38 S. F. Boys and F. Bernardi, *Mol. Phys.*, 1970, **19**, 553.
39 Y. Liu, M. Suhm and P. Botschwina, *Phys. Chem. Chem. Phys.*, 2004, **6**, 4642.
40 P. Botschwina, T. Dutoi, M. Mladenović, R. Oswald, S. Schmatz and H. Stoll, *Faraday Discuss.*, 2001, **118**, 433.
41 P. Botschwina and H. Stoll, *Phys. Chem. Chem. Phys.*, 2001, **3**, 1965.